The Future of Our Local Interstellar Medium

Ryland Brooks [a]
August 10, 2006

ABSTRACT

Analysis of a high resolution spectroscopy survey of 43 nearby stars in the direction of our solar trajectory through the galaxy. The spectra were taken with either the McDonald Observatory 2.7 m or the Anglo-Australian Observatory 3.4 m with a R between $\sim$ 60,000 and $\sim$ 1,000,000. The spectra were centered around either the Calcium H and K lines, located at 3968.4673 $\mathring{A}$ and 3933.6614 $\mathring{A}$ respectivly, or the Sodium D doublet, located at 5889.9510 $\mathring{A}$ and 5895.9242 $\mathring{A}$. A flux background was fit to each of the spectra and telluric absorption features were removed from the Sodium spectra. The absorption lines in these spectra are currently being used in a calculation of column density as a function of velocity along these near-solar-trajectory sightlines, giving us an understanding of the compostion of the Insterstellar Medium which we will be passing through over the next 3 to 30 million years.

1. Introduction

Space is not a vacuum. Although, for all intents and purposes, it is a vacuum, when looked at on the right scale, it is practically teeming with matter. Beyond the obvious planets and stars, there is a plethora of matter collectively referred to as the Interstellar Medium (ISM). The relative abundances of different elements and molecules comprising the ISM is not dissimilar to the familiar percentages quoted for the make up of the rest of the baryonic universe, and for good reason. The ISM is what stars and planets are born from and what, when they die, they will disperse back into. Most of the matter in the ISM (about 99%) is in a gaseous state, with about 90% by mass in one form of hydrogen or another. The remaining 10% is mostly helium leaving just a few percent for all other elements. There are also traces of complex molecules and interstellar dust floating through the medium, adding even more complexity to the system.

The composition of the Interstellar Medium immediately surrounding our solar system, referred to as Local Interstellar Medium (LISM), has been researched extensively and even mapped. Additionally, it is now known that this composition greatly affects the radius of our sun's heliosphere, our solar system's main defense against cosmic rays streaming through our galaxy[1]. It is

[a]email: rtbrooks@colby.edu

[1]There are also extragalactic cosmic rays of a much higher energy, but these are more pertinent in the study of

understood that the radius of the heliosphere, a boundary of ionized gas where our sun's outward radiation pressure reaches equilibrium with the ambient pressure of the LISM, has a far greater dependence on the pressure and density of the LISM environment which we are in than on the cyclic fluctuations of our sun's luminal output. Also, looking around the general ISM reveals large density variations, up to six orders of magnitude in some places (Redfield, 2006). This implies that by looking at the composition of our past or future LISM we should be able to make connections or predictions about the state of the heliosphere. The heliosphere currently extends to around 100 AU from our sun, comfortably fitting our entire solar system inside[2], but it is not difficult to imagine a LISM scenario where it would be compressed to a radius of below 1 AU. A loss of protection by our heliosphere would result in an increase of cosmic ray incidences on Earth of up to two orders of magnitude. It is widely accepted that cosmic rays serve as a prominent natural source of mutation in organisms, comprising 30 - 40 % of our annual natural dose of radiation in the form of muons, produced by cosmic ray events in the upper atmosphere. These incidences cause showers of muons and other charged particles that rain down to the lower atmospheric levels and earth. These charged particles are known to act as cloud nucleation sites, forming low altitude cloud cover, produce NO and NO_2, which make quick work of ozone molecules, and possibly even trigger lightning strikes. Furthermore, it is thought that an increase in interstellar dust pollution in our atmosphere could easily result in a reverse greenhouse effect, working to block visible wavelengths of light from reaching the surface of the planet, severely altering our planetary albedo (Redfield, 2006). It is highly apparent that cosmic rays greatly effect the climate and inhabitants of this planet on a very fundamental level, and further apparent that the nature of our LISM is the main decisive factor in determining the magnitude of the cosmic ray flux we recieve. Therefor, knowledge of the composition of our future LISM would, in essence, be knowledge of the future of the climate and life on our planet; in other words a very long range weather report for Earth.

2. Observations

With this background motivating the study of our future LISM, a spectroscopic survey of 43 stars was taken in the direction or our future solar trajectory. Absorption spectra of the stars were taken at extremely high resolution over the course of many nights between the spring of 2004 and spring of 2006 on the McDonald Observatory Harlan J. Smith 2.7 m telescope and the Anglo-Australian 3.9 m telescope. Resolution from R $\sim$ 60,000 to R $\sim$ 1,000,000[3] was used to

---

the galactic halo, wind and termination shock. The cosmic rays that are referred to in this paper have energies on the order of < 1 GeV.

[2]our solar system has a radius of approximately 39 AU, whereas the radius of the heliosphere in the upwind direction is approximately 94 AU.

[3]Instrumentation at McDonald Observatory: CS12: Coudé double-pass Spectrometer (R $\sim$ 500,000); CS21: Cross-Dispersed Echelle Spectrometer (2D Coudé) Focus 1 (R $\sim$ 240,000); CS23: Cross-Dispersed Echelle Spectrometer (2D Coudé) Focus 3(R $\sim$ 60,000); Instrumentation at the Anglo-Australian Observatory: UHRF: Ultra High Resolution

obtain high signal-to-noise spectra of these 43 sources. The stars in the survey were selected on the basis of their high brightness and their proximity both to our sun and to the exact direction of the future motion of our sun along the galactic plane. The stars have visual magnitudes between 9.0 and 3.9 and are of various spectral classes. The closest star to us is $44.1^{+1.5}_{-1.4}$ pc away while the farthest is 382^{+589}_{-144} pc away[4]. Our solar system is traveling at a rate of approximately 1 pc every 73,000 years, meaning that the stars in the survey are in the LISM environment that we will experience from about 3,000,000 years from now until about 28,000,000 years from now. The largest angular separation between our actual trajectory and the direction to any of the stars in the survey is only 9.89° of galactic coordinates. The spectra were taken to look for Calcium H and K[5] and the Sodium D lines[6]. These strong absorption features should be present and fairly evenly distributed in the ISM, effectively tracing ionized gas, making them helpful mapping tools. The method being used to map our future LISM is to look at what absorptions are detected where, ultimately working toward calculating column density along the sight line to each of the stars as a function of gas velocity. Identification of the different regions of ISM present is fairly straightforward due to density variations and Doppler shifting of the absorptions from the motion of the gas. Confusing stellar Calcium H and K and Sodium D lines with those from the ISM is also a non-issue because of the extreme smearing our of the stellar lines caused by the relatively rapid rotation of stars compared to the motion of the ISM.

The data was reduced by S. Redfield, the P.I. on the project and my adviser, prior to its presentation to me. Each spectra had already been coadded, calibrated and converted into an IDL save-set containing three vectors; wavelength in Angstroms, flux in ADUs and the error in that flux.

3. Analysis

The ultimate goal of the analysis was to get the spectra into a form from which column density along each of the 43 sight-lines could be calculated. Column density will ultimately be calculated by the Apparent Optical Depth method, as described by Savage & Sembach (1991). To get the spectra to this stage, however, a number of intermediate analysis steps had to be taken first, as described below.

Tables of stellar parameters were compiled, listing the information by source, followed by tables of observational parameters and data, organized by observation. Signal to noise values for each of the spectra were calculated and are included in the latter. These tables are included as Table 1 and

---

Facility (R ∼ 1,000,000).

[4]All stellar parameters are quoted from SIMBAD.

[5]Centered at 3968.4673 $\AA$ and 3933.6614 $\AA$ respectively.

[6]Centered at 5889.9510 $\AA$ and 5895.9242 $\AA$.

Table 2 at the end of this document. The spectra also all had to be cropped and pieced together because they were presented in the separate echelle orders. Going through all of the files, the order containing the absorption features was found and written into a separate save-set.

Plots of the positions of the stars on the sky were an important feature of the analysis, helping to keep track of where the stars and ISM in the survey were located. Two different types of plots were made. A two dimensional scatter plot which depicts the stars on the sky with the intersection point of the x and y axes at the point of our trajectory and the axes scaled in degrees of galactic coordinates, ℓ and b. The points representing the relative positions of the stars were scaled so their size was inversely proportional to the distance the star is from our sun and the HD numbers of the stars were printed in small text across the points. This is an extremely helpful tool in determining and keeping track of the distribution of the stars on the sky and through space. This plot is included as Figure 1. A second plot was made, scatter-plotting the position of the sources in three dimensions. The x axis was scaled to degrees of ℓ, the y axis as distance from our sun in pc and the z axis as degrees of b. It is important to note that one must take care in reading this plot because,in the x - z plane, it is a cubic representation of a spheric coordinate system. Instead of attempting to read the points on the cubic scale, one must imagine concentric circles superimposed onto the plot and interpolate positions off of this. The points were then given a variety of colors, to make them easily discernible from one another, and lines were drawn perpendicularly down from the point to the x - y plane. This plot, included as Figure 2, was another useful tool in looking at the stars' distribution through space.

Each spectra had a flux background fit to it and then divided out, normalizing the spectrum. This process removed any background continuum that the spectra had. This is a quality of the spectra that differs from CCD to CCD due to inherent differences in instrumental response. Without removing this continuum it there would be no common gorund from which to compare the various spectra, rendering it impossible to determine the relative strengths of the lines from source to source. The fitting was done using a IDL procedure written by S. Redfield, and proved to be very time consuming. It worked by allowing the user to select areas of background, fitting a polynomial of an order determined by the user to it, then interpolating what the line between those areas should look like. For the NaI spectra, an additional step, determining the number of sigma away from the line the procedure should reject, was made necessary by the high quantity of telluric features in that region. Without adding in a sigma rejection, the procedure would attempt to fit all of the numerous telluric lines, throwing off the entire fit. After having the background fit and divided out, each spectra was once again saved as a new save-set.

The next step was to go through each of the NaI spectra and attempt to remove as much of the telluric interference as possible. Without doing this it was often extremely difficult to determine which of the peaks in the spectra the D lines were. Because of Doppler shifting the lines were not exactly where they would have been in a laboratory setting, and it is exactly that shift that both aided in finding and extracting the lines and will ultimately show how the ISM is moving. The telluric removal procedure worked by using a model of the atmosphere to produce a mock spectral

energy distribution of just the telluric absorptions. The model was then modified to simulate what it would look like when put through each of the four different spectroscopic setups used in this survey. The procedure looked to remove this model sky, checking for the NaI absorptions in velocity space. Because the two absorptions from NaI were being created by the same ions of sodium, and thus moving at the same velocity, the two lines would have to be Doppler shifted by the same amount from their laboratory wavelengths. If the wavelength vector in the save-set is converted into two velocity vectors, zeroing the vector at the wavelength of each of the two laboratory values for the absorptions and saving them as separate vectors, then, when plotted against flux, the two NaI absorption features will line up. All other noise, patterns, telluric features or anything else will just be a random jumble, unable to line up because, in velocity space, they are not shifted from the zero point of the two NaI features by the same amount. Using this method, velocity estimates can also be obtained for the gas by looking at the velocity of the shifted peak. No shift would mean the cloud was moving at the same velocity as our solar system, a positive shift would mean the cloud is moving slower and a negative shift would indicate that the cloud is moving faster. Unfortunately, because we are working with Doppler shifts, only components of motion along the direction of the sight-line can be detected, however, as will be discussed later, there are other ways to detect other motion. Using this method, the procedure was able to coax most of the telluric features out of the majority of the spectra. In some spectra, the features were only weakened by the procedure, but they were still a good deal better than they had been before running it.

The step following this was to use the Apparent Optical Depth method to calculate column density along the sight-line to each of the sources as a function of velocity. This method requires that each of the absorptions to be analyzed come in a pair, which is exactly the case with both NaI and CaII. The absorption lines are converted into apparent optical depth by the equation,

$$\tau_a(v) = \ln\left[\frac{I_0(v)}{I_{obs}(v)}\right] \tag{1}$$

and the various measurements of $\tau_a(v)$ are then converted into apparent column density per unit of velocity, $N_a(v)$, using the equation,

$$\log\left[N_a(v)\right] = \log\tau_a(v) - \log\left(f\lambda\right) + 14.576 \tag{2}$$

in units of atoms cm^{-2} (km s^{-1}) where $N_a(v)$ is the number density in the column per unit velocity. The accuracy of this method is strongly contingent on three assumptions about the spectra being analyzed. First, the instrumental resolution must be high compared to the line width of the signal. Second, there must be a high signal to noise quotient and third, the level of background flux continuum must be well defined. Fortunately, our spectra fit all of these criteria. They are extremely high resolution, they have very good signal to noise and they have been normalized, removing most all of the continuum.

An IDL procedure, also written by S. Redfield, to do the calculations was provided to me and I was able to run this procedure on a large portion of the spectra in the time remaining. I am just now completeing the preliminary set of calculations for all of the observations, producing the

initial set of pieces that now need to be arranged into a readable puzzle. What we expect to see is an increase in the density of the ISM starting along the edge of the local bubble, however the extent of this increase is still unknown. It is too early in the process to draw conclusions on what our future LISM environment has in store for us, but I will continue working on this project as the coming academic year begins under my advisor at Colby College. We have now reached the most exciting point of the project; years of observations, reduction and analysis are culmiinating in these final steps, allowing us, for the first time, to catch a glimpse into the future of our planet and every living thing on it.

4. Future Work

The current step in the project is to complete the calculations of column density as described above. Once this is finished the result will be a five dimensional map[7] of where the ISM in this region is, what its approximate density is and what its velocity distribution looks like.

Beyond this, however, these is a great deal of work that can still be done to further our knowledge of the system. If more spectra are taken of the same sources and other bright sources within the vicinity of the original 43, it should be feasible to see motion of some of the closer clouds of ISM. The current step of mapping out the ISM in this area will be essential to this next step, so that it can be determined where the closer clouds are. Once this is determined, though, any components of motion along the axis perpendicular to the sight-line would show up in variations in the measurements of the column density along said sight-line. It is important that the cloud is among the closer sources, for it should, in that case, subtend a greater arc on the sky and therefor be easier to detect motion in. The velocity distribution of the gas in these ions should be within the bounds of $\pm$ 100 km s^{-1} and therefor would be less detectable at larger distances.

[7]Three spacial dimensions, a fourth dimension of velocity and a fifth dimension of density.

5. Figures and Tables

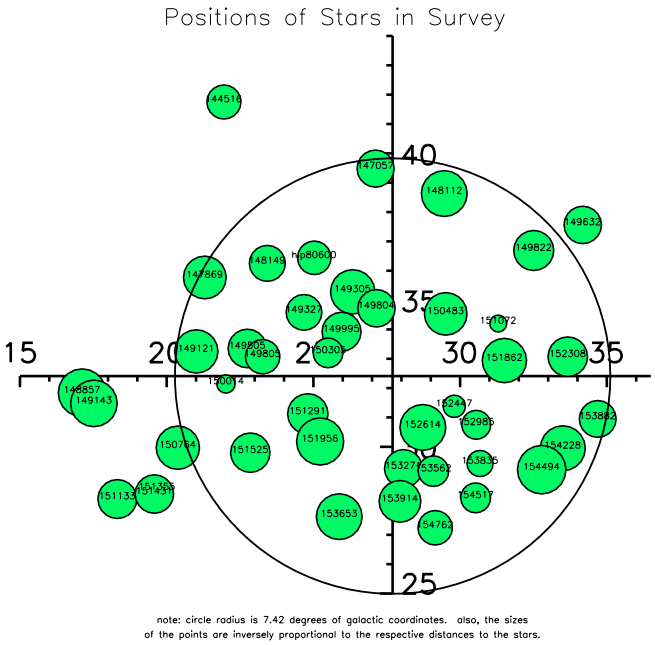

Fig. 1.— A plot of the position of the stars listed in table 1.

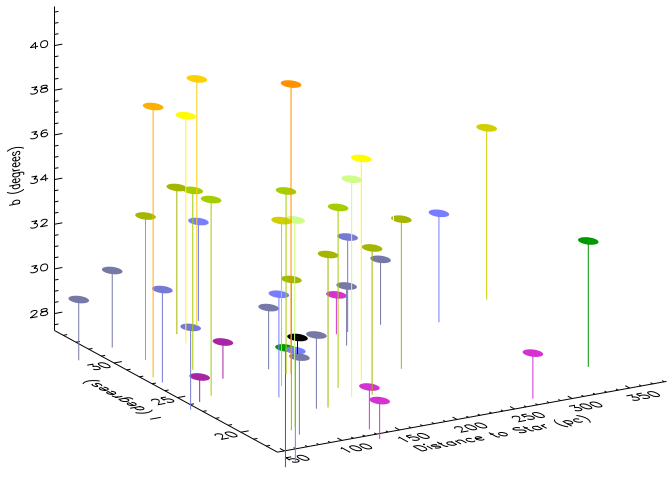

Fig. 2.— A scatter plot of the stars' positions on the sky and distances from our sun.

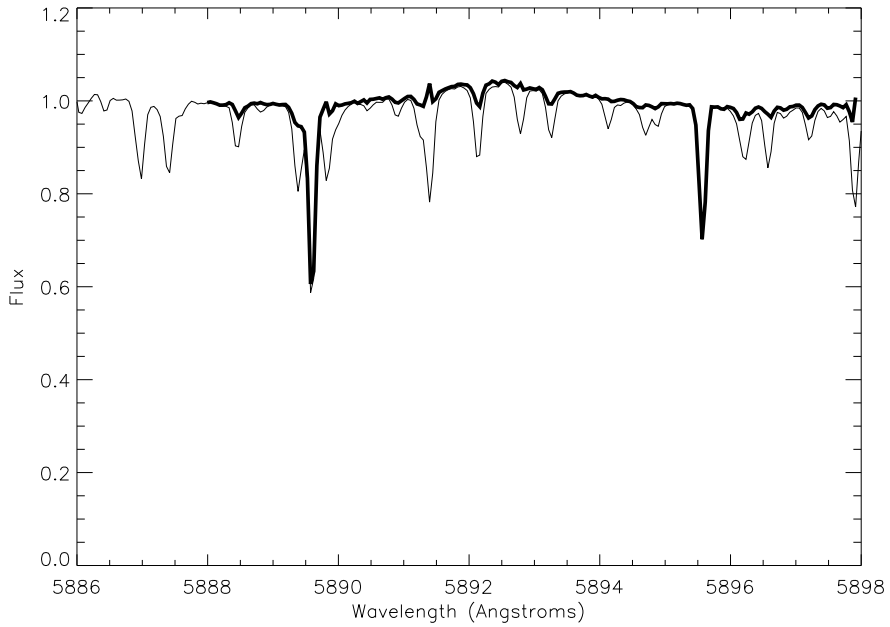

Fig. 3.— A plot of Flux versus Wavelength for the NaI lines of the LISM on the sightline of the star HD150764. The lighter line is original spectrum, full of telluric absorption features. The darker line is the spectrum after telluric feature removal was proformed.

Table 1. Stellar Parameters for Targets along the Future Solar Trajectory

HD #	Other Name	Spectral Type	m_v (mag)	v_R (km s^{-1})	$v \sin i$ (km s^{-1})	ℓ (°)	b (°)	Distance [a] (pc)	$\Delta\,\Theta$ [b] (°)
HD 144516	HIP 78858	A2	7.0	–34.6	···	21.95	+41.17	198^{+44}_{-30}	9.89
HD 147057	HIP 79947	A5	8.6	···	···	27.12	+39.48	166^{+46}_{-30}	7.0
HD 147869	21 Her	A2sp...	5.8	–33.4	65	21.30	+35.77	$104.7^{+8.7}_{-7.4}$	6.27
HD 148112	Ω Her	B9p...	4.6	–5.9	50	29.46	+38.63	$72.1^{+5.2}_{-4.6}$	6.38
HD 148149	HIP 80481	A2	8.9	···	···	23.43	+36.25	178^{+58}_{-35}	5.12
HD 148857	λ Oph	A0V+...	3.9	–13.5	138	17.12	+31.84	$50.9^{+3.7}_{-3.3}$	8.97
HD 149121	ν Her	B9.5iii	5.6	–27	16	21.01	+33.25	$98.8^{+10}_{-8.4}$	5.68
HD 149143	HIP 81022	G0	7.9	···	···	17.52	+31.48	$63.5^{+4.6}_{-4.0}$	8.68
HD 149305	HIP 81073	A3	6.8	+4	···	26.34	+35.28	$88.4^{+6.7}_{-5.8}$	3.08
HD 149327	HIP 81081	A2	8.1	···	···	24.68	+34.58	180^{+43}_{-29}	3.32
HD 149505	HIP 81189	A3	8.2	···	···	22.75	+33.35	150^{+31}_{-22}	4.26
HD 149632	HR 6169	A2V	6.4	–8.9	40	34.18	+37.56	162^{+27}_{-20}	7.39
HD 149804	HIP 81341	F0	7.8	–36.7	···	27.15	+34.72	162^{+30}_{-22}	2.36
HD 149805	γ Her	B9	7.3	–7.9	···	23.27	+33.07	194^{+41}_{-29}	3.78
HD 149882	V773 Her	B9sp...	6.4	+0.0	65	32.51	+36.69	134^{+16}_{-13}	5.83
HD 149995	HIP 81430	A2	8.1	–55.3	···	25.96	+33.92	145^{+24}_{-18}	2.10
HD 150014	HIP 81452	A0	8.9	···	···	22.02	+32.14	368^{+322}_{-117}	4.81
HD 150305	HIP 81600	A2	8.4	···	···	25.50	+33.20	244^{+94}_{-53}	2.01
HD 150483	HR 6203	A3Vn	6.1	–32	254	29.51	+34.53	$106.6^{+9.3}_{-7.9}$	2.60
HD 150764	HIP 81846	A5	7.4	···	···	20.38	+29.97	99^{+13}_{-11}	6.72
HD 151072	HIP 81958	A0	8.6	–41.5	···	31.30	+34.20	382^{+589}_{-144}	3.50
HD 151133	16 Oph	B9.5iii	6.0	–13	70	18.32	+28.22	146^{+22}_{-17}	9.11
HD 151291	HIP 82104	A3	8.7	···	···	24.81	+31.12	130^{+27}_{-19}	2.78
HD 151355	HIP 82133	B8	8.8	···	···	19.67	+28.54	294^{+203}_{-85}	7.93
HD 151431	19 Oph	A3V	6.1	–6.2	159	19.58	+28.39	151^{+24}_{-18}	8.07
HD 151525	V776 Her	B9p...	5.2	–16.1	40	22.85	+29.80	141^{+20}_{-15}	4.90
HD 151862	HR 6246	A1V	5.9	–23.3	81	31.51	+32.94	$88.2^{+6.7}_{-5.8}$	3.25
HD 151956	κ Her	A3m	5.5	–3.6	47	25.23	+30.18	$57.8^{+2.7}_{-2.5}$	3.07
HD 152308	V823 Her	B9.5p...	6.5	–22.8	104	33.67	+33.07	139^{+17}_{-14}	5.06
HD 152447	HIP 82586	A0	8.0	–39.9	···	29.80	+31.38	324^{+157}_{-80}	2.06
HD 152614	ι Oph	B8V	4.4	–21	110	28.73	+30.66	$71.7^{+3.9}_{-3.5}$	1.96
HD 152985	HIP 82890	A2	9.0	···	···	30.55	+30.75	253^{+105}_{-57}	2.94
HD 153271	HIP 83037	F0	8.3	···	···	28.07	+29.26	157^{+46}_{-29}	3.17
HD 153562	HIP 83178	A0	7.4	···	···	20.09	+29.17	236^{+60}_{-40}	7.29
HD 153653	HR 6317	A7V	6.6	–10	170	25.88	+27.63	$73.1^{+5.0}_{-4.4}$	5.03
HD 153835	HIP 83299	A0	7.7	···	···	30.68	+29.43	283^{+103}_{-60}	3.93
HD 153882	V451 Her	B9p...	6.3	–32.4	27	34.69	+30.95	169^{+24}_{-19}	6.12

Table 1—Continued

HD #	Other Name	Spectral Type	m_v (mag)	v_R (km s^{-1})	$v \sin i$ (km s^{-1})	ℓ (°)	b (°)	Distance [a] (pc)	$\Delta\,\Theta$ [b] (°)
HD 153914	HR 6329	A4V	6.4	+6.1	133	27.95	+28.14	116^{+19}_{-14}	4.28
HD 154228	HR 6341	A1V	5.9	–31.7	43	33.50	+29.95	$80.8^{+4.8}_{-4.3}$	5.54
HD 154494	60 Her	A4iv	4.9	–4.2	117	32.78	+29.22	$44.1^{+1.5}_{-1.4}$	5.40
HD 154517	HIP 83634	A5	8.4	···	···	30.53	+28.26	243^{+180}_{-72}	4.81
HD 154762	HIP 83764	B9	7.3	–13.9	···	29.15	+27.24	194^{+48}_{-32}	5.32
···	HIP 80600	F2	8.7	···	···	25.03	+36.44	204^{+66}_{-40}	4.59

[a]Distances calculated from parallaxes quoted by SIMBAD.

[b]Angular distance from the future solar trajectory, $\ell = 27.70°$, $b = +32.41°$.

Note. — All values from SIMBAD unless otherwise noted.

Table 2. Observational Parameters for Targets along the Future Solar Trajectory

HD #	Other Name	Date	Telescope [a]	Instrument [b]	Ion	Exposure (s)	S/N
HD 148112	Ω Her	2004 Apr 6	McD2.7	CS12	CaII	···	38
HD 148112	Ω Her	2004 Apr 7	McD2.7	CS12	CaII	···	54
HD 152614	ι Oph	2004 Apr 7	McD2.7	CS12	CaII	···	52
HD 152614	ι Oph	2004 Oct 18	McD2.7	CS21	CaII	···	56
HD 152614	ι Oph	2004 Oct 18	McD2.7	CS21	NaI	···	60
HD 148857	λ Oph	2004 Oct 19	McD2.7	CS21	CaII	···	45
HD 148857	λ Oph	2004 Oct 19	McD2.7	CS21	NaI	···	231
HD 151525	V776 Her	2004 Oct 19	McD2.7	CS21	NaI	···	115
HD 151525	V776 Her	2004 Oct 19	McD2.7	CS21	CaII	···	14
HD 148857	λ Oph	2004 Oct 19	McD2.7	CS12	CaII	···	45
HD 148857	λ Oph	2004 Oct 19	McD2.7	CS12	CaII	···	230
HD 144516	HIP 78858	2004 Oct 20	McD2.7	CS21	NaI	···	29
HD 144516	HIP 78858	2004 Oct 20	McD2.7	CS21	CaII	···	6
HD 154494	60 Her	2004 Oct 20	McD2.7	CS21	CaII	···	···
HD 154494	60 Her	2004 Oct 20	McD2.7	CS21	NaI	···	50
HD 148112	Ω Her	2004 Oct 21	McD2.7	CS21	CaII	···	40
HD 148112	Ω Her	2004 Oct 21	McD2.7	CS21	NaI	···	≤ 11
HD 152308	V823 Her	2005 Apr 18	McD2.7	CS23	CaII, NaI	···	229, 700
HD 149805	γ Her	2005 Apr 18	McD2.7	CS23	CaII, NaI	···	183, 580
HD 154762	HIP 83764	2005 Apr 18	McD2.7	CS23	CaII, NaI	···	185, 587
HD 149121	ν Her	2005 Apr 19	McD2.7	CS23	CaII, NaI	···	229, 862
HD 149995	HIP 81430	2005 Apr 19	McD2.7	CS23	CaII, NaI	···	··· , 391
HD 150305	HIP 81600	2005 Apr 19	McD2.7	CS23	CaII, NaI	···	40, 153
HD 149822	V773 Her	2005 Apr 20	McD2.7	CS23	CaII, NaI	···	195, 581
HD 150305	HIP 81600	2005 Apr 20	McD2.7	CS23	CaII, NaI	···	37, 154
HD 149305	HIP 81073	2005 Apr 20	McD2.7	CS23	CaII, NaI	···	150, 536
HD 152447	HIP 82586	2005 Apr 20	McD2.7	CS23	CaII, NaI	···	87, 284
HD 151355	HIP 82133	2005 Apr 21	McD2.7	CS23	CaII, NaI	···	105, 249
HD 149327	HIP 81081	2005 Apr 21	McD2.7	CS23	CaII, NaI	···	73, 337
HD 151291	HIP 82104	2005 Apr 21	McD2.7	CS23	CaII, NaI	···	73, 270
HD 154228	HR 6341	2005 Jun 12	AAT3.9	UHRF	CaII	···	10
HD 152614	ι Oph	2005 Jun 20	McD2.7	CS23	CaII, NaI	···	90, 285
HD 151072	HIP 81958	2005 Jun 20	McD2.7	CS23	CaII, NaI	···	24, 132
HD 152985	HIP 82890	2005 Jun 20	McD2.7	CS23	CaII, NaI	···	8, 96
HD 151525	V776 Her	2005 Jun 21	McD2.7	CS23	CaII, NaI	···	93, 279
HD 149505	HIP 81189	2005 Jun 21	McD2.7	CS23	CaII, NaI	···	75, 212
HD 153562	HIP 83178	2005 Jun 21	McD2.7	CS23	CaII, NaI	···	8, 121

Table 2—Continued

HD #	Other Name	Date	Telescope [a]	Instrument [b]	Ion	Exposure (s)	S/N
HD 148112	Ω Her	2005 Jun 23	McD2.7	CS23	CaII, NaI	···	140, 469
HD 154517	HIP 83634	2005 Jun 23	McD2.7	CS23	CaII, NaI	···	50, 251
HD 153653	HR 6317	2005 Jun 23	McD2.7	CS23	CaII, NaI	···	18, 234
HD 153882	V451 Her	2005 Jun 29	McD2.7	CS23	CaII, NaI	···	195, 594
HD 147057	HIP 79947	2005 Jun 29	McD2.7	CS23	CaII, NaI	···	100, 345
HD 150764	HIP 81846	2005 Jun 29	McD2.7	CS23	CaII, NaI	···	150, 616
HD 149804	HIP 81341	2005 Jun 29	McD2.7	CS23	CaII, NaI	···	48, 514
HD 153271	HIP 83037	2005 Jun 29	McD2.7	CS23	CaII, NaI	···	49, 346
HD 153835	HIP 83299	2005 Jun 29	McD2.7	CS23	CaII, NaI	···	90, 359
HD 148149	HIP 80481	2005 Jun 29	McD2.7	CS23	CaII, NaI	···	8, 115
HD 154494	60 Her	2005 Jun 30	McD2.7	CS23	CaII, NaI	···	320, 1078
···	HIP 80600	2005 Jun 30	McD2.7	CS23	CaII, NaI	···	200, 310
HD 148149	HIP 80481	2005 Jun 30	McD2.7	CS23	CaII, NaI	···	132, 458
HD 150014	HIP 81452	2005 Jun 30	McD2.7	CS23	CaII, NaI	···	44, 201
HD 150483	HR 6203	2005 Jun 30	McD2.7	CS23	CaII, NaI	···	90, 332
HD 148857	λ Oph	2005 Jun 30	McD2.7	CS23	CaII, NaI	···	100, 625
HD 152308	V823 Her	2005 Jun 30	McD2.7	CS23	CaII, NaI	···	25, 122
HD 152308	V823 Her	2005 Jul 15	McD2.7	CS21	CaII	···	40
HD 152308	V823 Her	2005 Jul 15	McD2.7	CS21	NaI	···	92
HD 154228	HR 6341	2005 Jul 16	McD2.7	CS21	CaII	···	35
HD 154228	HR 6341	2005 Jul 16	McD2.7	CS21	NaI	···	137
HD 149121	ν Her	2005 Jul 16	McD2.7	CS21	NaI	···	123
HD 149121	ν Her	2005 Jul 16	McD2.7	CS21	CaII	···	40
HD 149822	V773 Her	2005 Jul 16	McD2.7	CS21	CaII	···	33
HD 149822	V773 Her	2005 Jul 16	McD2.7	CS21	NaI	···	75
HD 153882	V451 Her	2005 Jul 17	McD2.7	CS21	CaII	···	29
HD 153882	V451 Her	2005 Jul 17	McD2.7	CS21	NaI	···	90
HD 150483	HR 6203	2005 Jul 17	McD2.7	CS21	NaI	···	97
HD 150483	HR 6203	2005 Jul 17	McD2.7	CS21	CaII	···	29
HD 151862	HR 6246	2005 Jul 17	McD2.7	CS21	CaII	···	30
HD 151862	HR 6246	2005 Jul 17	McD2.7	CS21	NaI	···	86
HD 151956	κ Her	2005 Jul 17	McD2.7	CS21	NaI	···	103
HD 151956	κ Her	2005 Jul 17	McD2.7	CS21	CaII	···	24
HD 148857	λ Oph	2005 Jul 18	McD2.7	CS12	CaII	···	63
HD 151525	V776 Her	2005 Jul 18	McD2.7	CS12	CaII	···	45
HD 152614	ι Oph	2005 Jul 18	McD2.7	CS12	CaII	···	75
HD 148112	Ω Her	2005 Jul 18	McD2.7	CS12	CaII	···	50

Table 2—Continued

HD #	Other Name	Date	Telescope [a]	Instrument [b]	Ion	Exposure (s)	S/N
HD 148857	λ Oph	2005 Jul 19	McD2.7	CS12	NaI	···	63
HD 151525	V776 Her	2005 Jul 19	McD2.7	CS12	NaI	···	49
HD 152614	ι Oph	2005 Jul 19	McD2.7	CS12	NaI	···	64
HD 148112	Ω Her	2005 Jul 19	McD2.7	CS12	NaI	···	39
HD 154494	60 Her	2005 Jul 19	McD2.7	CS12	NaI	···	28
HD 154494	60 Her	2005 Jul 20	McD2.7	CS12	CaII	···	36
HD 151133	16 Oph	2005 Jul 21	McD2.7	CS21	CaII	···	27
HD 151133	16 Oph	2005 Jul 21	McD2.7	CS21	NaI	···	50
HD 153914	HR 6329	2005 Sep 14	McD2.7	CS21	NaI	···	79
HD 153914	HR 6329	2005 Sep 14	McD2.7	CS21	CaII	···	22
HD 151525	V776 Her	2005 Sep 14	McD2.7	CS21	CaII	···	64
HD 151525	V776 Her	2005 Sep 14	McD2.7	CS21	NaI	···	96
HD 152614	ι Oph	2005 Sep 14	McD2.7	CS21	CaII	···	70
HD 152614	ι Oph	2005 Sep 14	McD2.7	CS21	NaI	···	128
HD 154494	60 Her	2005 Sep 14	McD2.7	CS21	NaI	···	98
HD 154494	60 Her	2005 Sep 14	McD2.7	CS21	CaII	···	51
HD 148112	Ω Her	2005 Sep 15	McD2.7	CS21	NaI	···	147
HD 148112	Ω Her	2005 Sep 15	McD2.7	CS21	CaII	···	57
HD 148857	λ Oph	2005 Sep 15	McD2.7	CS21	CaII	···	73
HD 148857	λ Oph	2005 Sep 15	McD2.7	CS21	NaI	···	177
HD 147869	21 Her	2005 Sep 15	McD2.7	CS21	NaI	···	66
HD 147869	21 Her	2005 Sep 15	McD2.7	CS21	CaII	···	21
HD 149632	HR 6169	2005 Sep 15	McD2.7	CS21	CaII	···	27
HD 149632	HR 6169	2005 Sep 15	McD2.7	CS21	NaI	···	73
HD 151431	19 Oph	2005 Sep 15	McD2.7	CS21	NaI	···	65
HD 151431	19 Oph	2005 Sep 15	McD2.7	CS21	CaII	···	17
HD 154494	60 Her	2006 Mar 19	AAT3.9	UHRF	CaII	···	9
HD 149143	HIP 81022	2006 Apr 8	McD2.7	CS23	CaII, NaI	···	58, 13
HD 149143	HIP 81022	2006 Apr 9	McD2.7	CS23	CaII, NaI	···	37, 232

[a]McD2.7: The Harlan J. Smith 2.7m Telescope at McDonald Observatory; AAT3.9: The Anglo-Australian 3.9m Telescope at the Anglo-Australian Observatory.

[b]CS12: Coudé double-pass Spectrometer (R $\sim$ 500,000); CS21: Cross-Dispersed Echelle Spectrometer (2D Coudé) Focus 1 (R $\sim$ 240,000); CS23: Cross-Dispersed Echelle Spectrometer (2D Coudé) Focus 3 (R $\sim$ 60,000); UHRF: Ultra High Resolution Facility (R $\sim$ 1,000,000).

6. References

Frisch, P.C., "Solar Journey: The Significance of Our Galactic Environment For The Heliosphere and Earth", page 1 - 22, Springer, 2006

Redfield, S., 2006, ASP, Frank N. Bash Symposium 2005: New Horizons in Astronomy, "The Local Interstellar Medium"

Redfield, S., Linsky, J.L., 2002, ApJ, 139, 439-465, "The Structure of The Local Interstellar Medium. I. High-Resolution Observations of Fe II, Mg II, and CaII Toward Stars Within 100 Parsecs"

Savage, B.D., Sembach, K.R., 1991, ApJ, 379, 245-259, "The Analysis Of Apparent Optical Depth Profiles For Interstellar Absorption Lines"